Supplementary Information

All-Electrical Layer-Spintronics in Altermagnetic Bilayer

Rui Peng,[1,*] Jin Yang,[1,2] Lin Hu[3,4,5], Wee-Liat Ong,[2] Pin Ho,[6] Chit Siong Lau,[1,6]

Junwei Liu[7], Yee Sin Ang[1,*]

[1]Science, Mathematics and Technology (SMT) Cluster, Singapore University of Technology and Design, Singapore 487372

[2]ZJU-UIUC Institute, College of Energy Engineering, Zhejiang University, Jiaxing, Haining, Zhejiang, 314400, China

[3]Centre for Quantum Physics, Key Laboratory of Advanced Optoelectronic Quantum Architecture and Measurement (MOE), School of Physics, Beijing Institute of Technology, Beijing 100081, China

[4]Beijing Key Lab of Nanophotonics & Ultrafine Optoelectronic Systems, School of Physics, Beijing Institute of Technology, Beijing 100081, China

[5]Beijing Computational Science Research Center, Beijing 100193, China

[6]Institute of Materials Research and Engineering (IMRE), Agency for Science, Technology and Research (A*STAR), Singapore 138634

[7]Department of Physics, Hong Kong University of Science and Technology, Hong Kong 999077, China.

*Corresponding authors: rui_peng@sutd.edu.sg; yeesin_ang@sutd.edu.sg

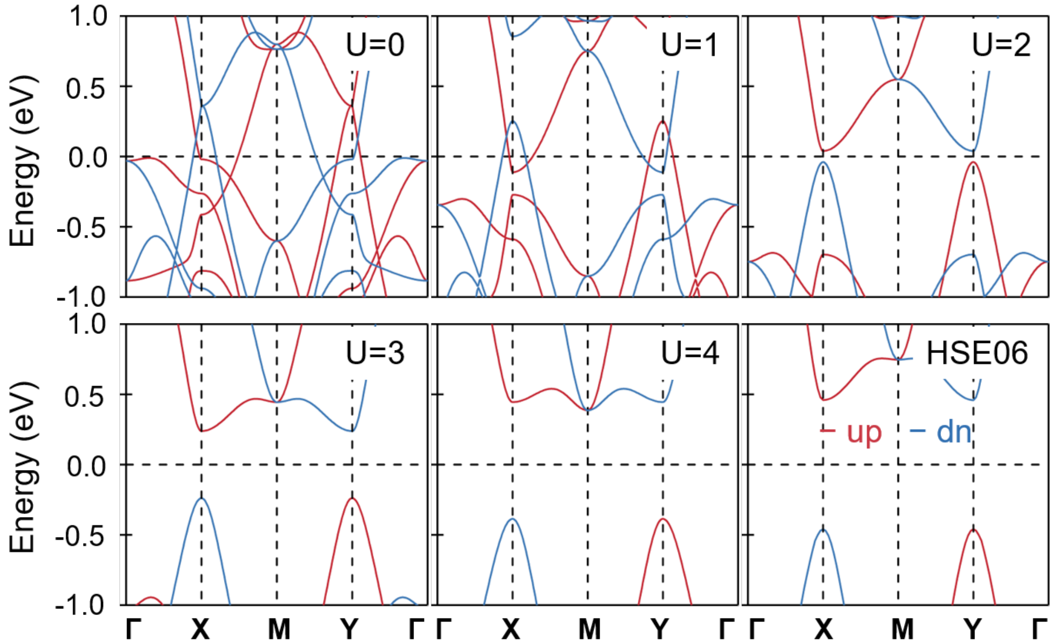

Fig. S1 Spin-polarized band structures of CrS monolayer using different effective Hubbard U_{eff} and HSE06. The Fermi level is set to the middle of the band gap.

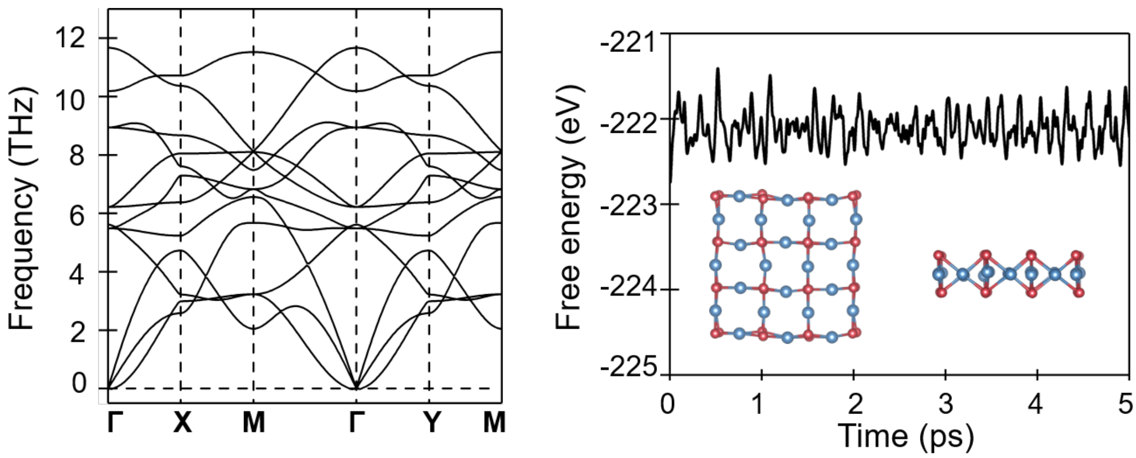

Fig. S2 (a) Phonon frequency spectrum of CrS monolayer. No imaginary modes appear in the phonon frequency spectrum. (b) Variations of the total energy of CrS monolayer at 300 K during AIMD simulations. Inset shows the snapshots of the equilibrium structure of CrS monolayer. Neither bond breakage nor structural reconstruction are observed in the snapshots after annealing for 5 ps.

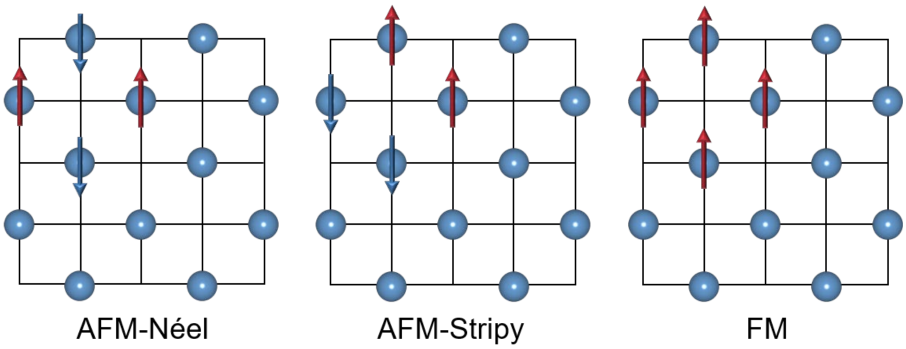

Fig. S3 Different magnetic configurations of CrS monolayer. The blue and red arrows indicate spin down and spin up, respectively.

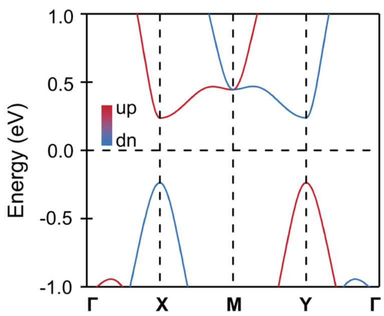

Fig. S4 Band structures of CrS monolayer with SOC. The Fermi level is set to the middle of the band gap.

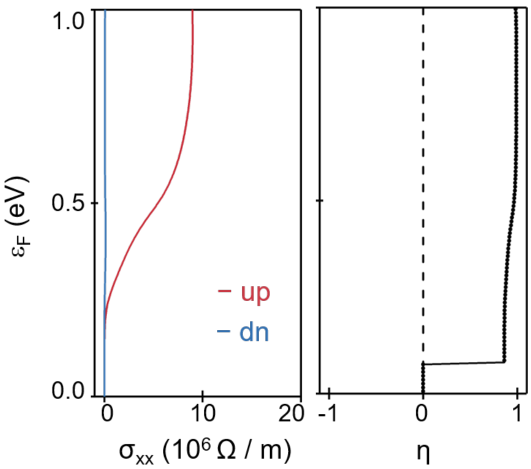

Fig. S5 Spin-resolved conductivity and spin polarization of the transport current in CrS monolayer.

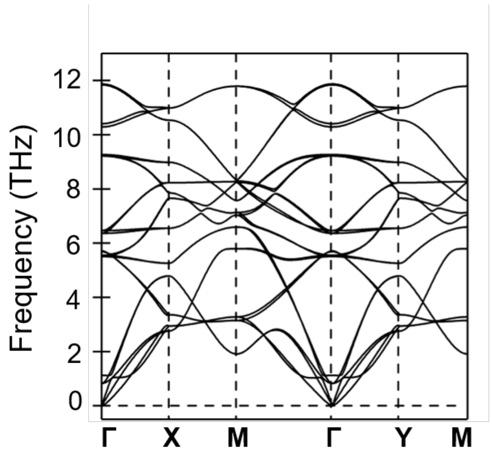

Fig. S6 Phonon frequency spectrum of CrS bilayer. No imaginary modes appear in the phonon frequency spectrum.

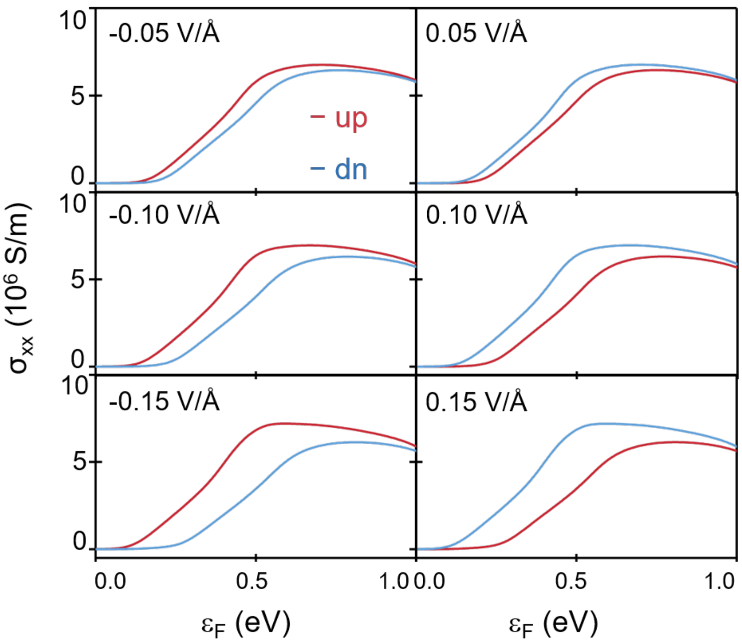

Fig. S7 Spin-resolved conductivity using the semi-analytical transport model based on the parabolic energy dispersion fitting of the CBMs of the layer-spin subbands at X and Y valleys under the out-of-plane electric field of ±0.05, ±0.10, and ±0.15 V/Å.

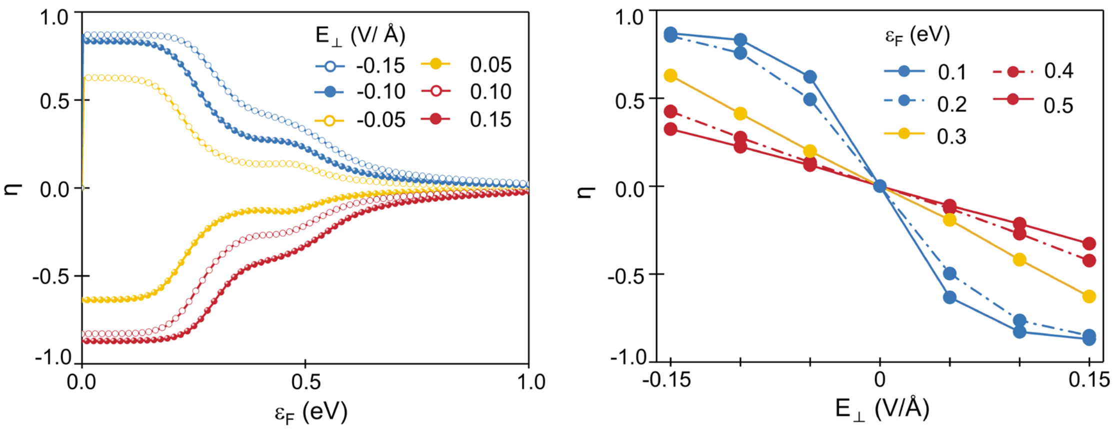

Fig. S8 Spin polarization of the transport current using the semi-analytical transport model based on the parabolic energy dispersion fitting of the CBMs of the layer-spin subbands at X and Y valleys as a function of Fermi level and out-of-plane electric field.

Electric field		AFM-Néel	AFM-Stripy	FM
In-plane	-0.15	0	0.48	1.31
	-0.10	0	0.48	1.31
	-0.05	0	0.48	1.31
	0.05	0	0.48	1.31
	0.10	0	0.48	1.31
	0.15	0	0.48	1.31
Out-of-plane	-0.15	0	0.48	1.30
	-0.10	0	0.48	1.30
	-0.05	0	0.48	1.30
	0.05	0	0.48	1.30
	0.10	0	0.48	1.30
	0.15	0	0.48	1.30

Table S1. Energy (eV) of AFM-Néel, AFM-Stripy and FM configurations of CrS monolayer under in-plane and out-of-plane electric field of ±0.05, ±0.10 and ±0.15 V/Å. The energy of AFM-Néel is set to 0.

Supplementary Notes

Based on Eq. 1, when T = 0 K, the conductivity tensor can be written as:

$$\sigma_{ij}^{V} = \frac{ne^2\tau}{m^*}$$

where n is the carrier density, and m* is the effective mass. m* can be presented as:

$$\left[\frac{1}{m^*}\right] = \frac{1}{\hbar^2}\begin{bmatrix} \frac{\partial^2 \varepsilon}{\partial k_x^2} & \frac{\partial^2 \varepsilon}{\partial k_x \partial k_y} \\ \frac{\partial^2 \varepsilon}{\partial k_y \partial k_x} & \frac{\partial^2 \varepsilon}{\partial k_y^2} \end{bmatrix}$$

Therefore, based on Eq. 2-3, the conductivity tensors at X and Y valleys can be written as:

$$\sigma_{ij}^{X} = \begin{bmatrix} \frac{ne^2\tau}{m_1} & 0 \\ 0 & \frac{ne^2\tau}{m_2} \end{bmatrix}$$

$$\sigma_{ij}^{Y} = \begin{bmatrix} \frac{ne^2\tau}{m_2} & 0 \\ 0 & \frac{ne^2\tau}{m_1} \end{bmatrix}$$

As we can see, the longitudinal conductivity at X and Y are $\sigma_{xx}^{X} = \frac{ne^2\tau}{m_1}$ and $\sigma_{xx}^{Y} = \frac{ne^2\tau}{m_2}$, respectively, and there is no transverse conductivity